2015 IEEE International Conference on
Automation Science and Engineering (CASE)
Aug 24-28, 2015. Gothenburg, Sweden

Visible Light Communication-based Indoor Environment Modeling and Metric-free Path Planning

Kejie Qiu, Fangyi Zhang
The Hong Kong University of Science and Technology
Email: {kqiuaa, eezhangfy}@ust.hk

Ming Liu
City University of Hong Kong
Email: mingliu@cityu.edu.hk

***Abstract*—For mobile robots and position-based services, localization is the most fundamental capability while path-planning is an important application based on that. A novel localization and path-planning solution based on a low-cost Visible Light Communication (VLC) system for indoor environments is proposed in this paper. A number of modulated LED lights are used as beacons to aid indoor localization additional to illumination. A Gaussian Process (GP) is used to model the intensity distributions of the light sources. Path-planning is hereby feasible by using the GP variance field, rather than using a metric map. Graph-based path-planners are introduced to cope with the practical situations. We demonstrate our path-planning system by real-time experiments performed on a tablet PC in an indoor environment.**

I. Introduction

A. Motivation

Precise localization is the fundamental capacity of many robotic applications and scenarios such as service and rescue robots. Also, localization information is one of the most essential data shared in a cloud robotic system [1]. Taking the visual approaches for example, FastSLAM has been widely applied [2] for laser range-finder-based mapping and path-planning. Efficient visual localization methods using omnidirectional cameras were introduced in our previous works [3], [4], [5], [6].

Based on the localization information, path-planning is a specific application, as it enables a robot to get to a defined goal position.

We propose to realize more robust and precise localization and path-planning by using modulated visible light to provide a stable global reference, where a cheap photonic diode is the only required sensor. The possibility of achieving accurate localization using such a system has been discussed in our previous work[7]. It supplies a low-cost practical solution for personal localization services, considering a photonic sensor is common on most consumer electronic devices. As a key to realize global localization, the details of codes selection for light modulation and decomposition method have been discussed in another previous work late last year [8].

The overall structure of the proposed approach is shown in Fig. 1. The mixed modulated light signal is captured by a photonic diode, which is decomposed using an ad-hoc blind signal decomposition algorithm. The signal intensity of each light source is further used for both environment modeling process and Bayesian filter-based localization. The environment model is represented by the mean fields and variance fields of the observed components. Using the real-time localization result, path-planning could be thus realized based on the variance fields.

This work was supported by the HKUST Project IGN13EG03; partially sponsored by the Research Grant Council of Hong Kong SAR Government, China, under project No. 16206014 and NSFC Youth Research Fund 6140021318.

B. Challenges and Contributions

There are several challenges in this work. Firstly, since we do not use exteroceptive sensors except a low-cost photonic diode, which is a sensor with scalar output, the environment modeling is challenging, because no metric information is readily available. Secondly, since we only have the observations from the photonic diode, precise localization is hard to achieve considering various observation situations, such as changed orientations of the sensor. Last, but not least, adaptive real-time path-planning needs the indoor map to be accurately constructed, which is usually a metric representation, which we do not have.

Despite these difficulties, the following contributions are addressed in this paper:

- We realize a data-driven environment modeling scheme based on Gaussian Process Regression using the scalar output from a photonic diode, such that no prior knowledge is required on the light distribution and indoor circumstance arrangement.
- We propose a novel idea for path-planning on the variance fields derived from the Gaussian Process. Real-time heuristic path-planning is achieved based on a projected cost-map from the variance field, which is validated by experiments.

C. Organization

Section II of this paper introduces different localization and path-planning solutions in the robotic areas, especially those based on VLC. In section III, we briefly introduce the construction of the VLC-based system and define the environment modeling and path-planning problem, including the I/O of the algorithm and application. Section IV introduces the scheme and implementation of the Gaussian Process-based environment modeling phase, followed by the illustration of different implementations of the path-planning algorithms using the former results of localization in Section V. Different path-planning algorithms are compared in the path-planning section. Finally, we make a conclusion of our work and envision future work.

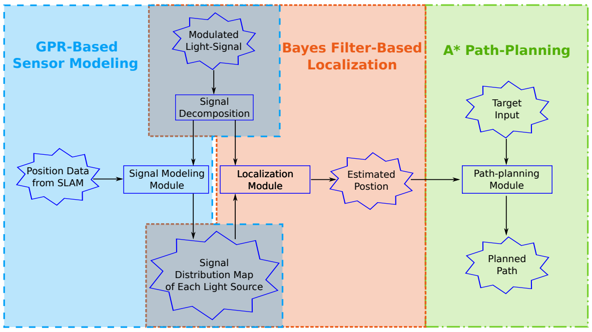

Fig. 1. The overall structure of the proposed solution for indoor localization

II. Related Work

A. Robotic Path-planning

The algorithms for path-planning have been well-studied, since lots of scientific and engineering problems can be summarized as finding an optimal path through a graph. Dijstra's algorithm is a widely used mathematical approach to find an overall minimum cost path by establishing a directed graph with cost defined between the connected nodes, which was firstly proposed by Dijkstra [9]. The computation feasibility is the first concern of this algorithm, although a prior queue may be adopted to reduce the computation complexity. A set of algorithms could be used to help improve the computation efficiency in the graph search process, such as heuristic methods. Hart introduced A* [10] to combine the information from a specific routing domain to realize a fast solution of path-planning. Modified versions of these basic methods have been widely applied [11], [12]. In this work, these existing path-planning algorithms will be compared using the localization result based on a Gaussian Process Regression model. The aforementioned algorithms perform re-planning at every single iteration, which is based on the fact that the environment model is completely constructed before the path is computed. In order to meet the need in partially known environments, D* [13], focused D* [14], and D*-Lite [15] were proposed. Colas *et al.* implemented the D*-Lite-based 3D path-planning on a multi-terrain robot for search and rescue missions [11]. Online path-planning on point-cloud was realized by Ming Liu on a local Riemannian metric based on the saliency components of tensor voting results [16].

B. Visible Light Communication (VLC)

VLC is a type of wireless communication technique, which makes use of visible light as the transmission medium of information. A key advantage of VLC is that it can be simultaneously used for illumination and communication. XW Ng et al. proposed a medical healthcare information system based on VLC, mainly considering the disturbance of electromagnetic waves to medical instruments [17]. Also, VLC could be used as a communication channel for autonomous control and remote manipulation [18], [19].

VLC-based positioning systems have also been discussed in literature [20]. However, most of these systems require several types of sensors to work together, such as the high-accuracy positioning system based on VLC proposed by M. Yoshino et al. [21], [22]. Although the system could measure both the position and direction of a receiver, it requires additional image processing procedures which would increase cost and time consumption. Kim *et al.* tried to overcome this disadvantage by using an intensity modulation/direct detection and radio frequency carrier allocation method [23], but the transmission channel consumption is relatively high in this case. Besides this, all of these methods require geometrical computation, rather than sensor data-driven modeling which has been proved to be sufficient for precise localization in our previous work [7].

III. Problem Definition

A typical setup is described as follows: in an indoor environment, several modulated LED tubes are distributed arbitrarily. Each LED has a unique modulation waveform, which is carefully selected to ensure high auto-correlation and low cross-correlation responses between every two tubes. Our demo VLC system is based on the previously proposed hardware as shown in Fig. 2 [7]. It emits white visible light

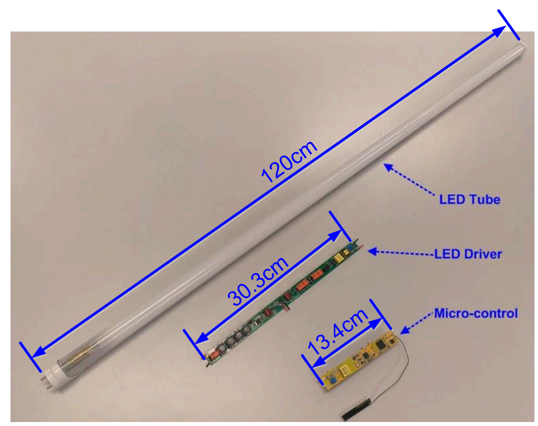

Fig. 2. VLC light sources used in this paper

using LEDs at a high frequency. A typical test environment using the hardware system is shown in Fig. 3, which replaces the original illuminant condition.

To get the light intensity vectors which describe the intensities of the components embedded in the received signal, a blind signal decomposition process is applied. Based on the known sensor locations and corresponding intensity vectors, the environment model could be represented as a set of intensity distribution maps in the test area aided by Gaussian Process. It results in two parts: the regression mean fields and the variance fields. The former represent the expected light signal observations; the latter represent the observation likelihoods.

In this paper, we mainly consider the path-planning module in the context of the VLC-based system. The objective of path-planning is to generate an optimal path in the map

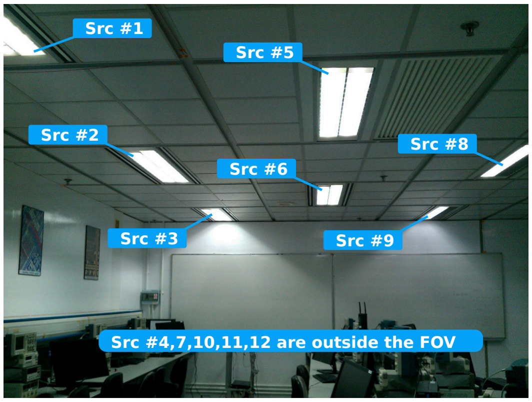

Fig. 3. A typical setup for the light sources of the VLC system

from the start position to a valid goal position. In order to use heuristic search algorithms, we have to convert the GP fields into structured cost-maps which contain nodes and arcs. Here we construct the cost-maps directly on the variance fields rather than on the maps generated by the mobile robot. An advantage is that an accurate map is no more a prerequisite for path-planning, which significantly reduces the requirements on map construction. Taking a position derived from the localization module, we label a destination on the map. By using path-planning methods, such as Dijkstra's algorithm and A* algorithm, we aim to find the optimal path with the minimum total cost based on the cost-map.

IV. Environment modeling

The VLC-based localization system mainly consists of two technical parts: Gaussian Process-based Modeling and Bayesian Filter-based localization. Since our path-planning solution is based on the variance field, which is part of the output of the modeling phase, we mainly discuss the environment modeling part in this paper.

To utilize the signal decomposition results, we need to model the luminous distribution of a certain room so that the specific location of each LED beacon is no longer needed once the indoor environment is determined, in other words, the localization works in a data-driven mode. Therefore, a data collection process is a prerequisite, which should be carefully arranged and cover all the possible operating area since the accurate localization and path-planning are only possible where the sensor has been in the data collection phase. After that, a Gaussian Process Regression model is applied to construct an environment model based on the decomposition results at different positions.

As for the Gaussian Process model, we follow the function-space definition described by Rasmussen [24]. Let $D = (\mathrm{x}_1, y_1), (\mathrm{x}_2, y_2), ..., (\mathrm{x}_n, y_n)$ be a set of training samples drawn from a noisy process

$$y_i = f(\mathrm{x}_i) + \varepsilon \tag{1}$$

where each x_i is an input sample in $\mathbb{R}^d$ and each y_i is an observation result in $\mathbb{R}$. ε is zero mean, additive Gaussian noise with known covariance σ_n^2. In practice, x_i denotes the 2D position and y_i denotes a component of the received signal. For notational convenience, we aggregate the n input vectors x_i into a $d \times n$ matrix X, and the target values y_i into the vector denoted y. A Gaussian Process estimates posterior distributions over functions f from training data D. These distributions are represented non-parametrically by using training samples. The key idea underlying GPs is the requirement that the function values at different positions are correlated, where the covariance between two function values, $f(\mathrm{x}_p)$ and $f(\mathrm{x}_q)$ are dependent on the input values x_p,x_q. This dependency can be specified via an arbitrary covariance function, or so-called kernel $k(\mathrm{x}_p, \mathrm{x}_q)$. The choice of the kernel function is typically left to the user, the most widely used being the squared exponential, or Gaussian kernel:

$$k(\mathrm{x}_p, \mathrm{x}_q) = \sigma_f^2 \mathrm{exp}(-\frac{1}{2l^2})|\mathrm{x}_p - \mathrm{x}_q|^2 \tag{2}$$

where σ_f^2 is the signal covariance and l is the length scale that determines how strongly the correlation between points maintains. Both parameters control the smoothness of the functions estimated by a GP. The covariance between function values decreases with the distance between their corresponding input vales.

Since we do not have direct access to the function values but only noisy observations, it is necessary to represent the corresponding covariance function for noisy observations:

$$\mathrm{cov}(y_p, y_q) = k(\mathrm{x}_p, \mathrm{x}_q) + \sigma_n^2 \delta_{pq} \tag{3}$$

where σ_n^2 is the Gaussian observation noise and δ_{pq} is one if $p = q$ and zero otherwise. For an entire set for input values X, the covariance over the corresponding observation y becomes

$$\mathrm{cov}(\mathrm{y}) = K + \sigma_n^2 I \tag{4}$$

where K is the $n * n$ covariance matrix of the input values, that is, $K[p, q] = k(x_p, x_q)$.

Note that for any set of values X, one can generate the matrix K and then sample a set of corresponding targets y that have the desired covariance. The sampled values are jointly Gaussian with $\mathrm{y} \sim N(0, K + \sigma_n^2 I)$. Additionally, it is the posterior distribution over functions given training data X, y. From Eq. 2 it follows that the posterior over function values is Gaussian with mean μ and covariance σ^2:

$$p(f(\mathrm{x}_*)|\mathrm{x}_*, X, y) = N(f(\mathrm{x}_*); \mu_{\mathrm{x}_*}, \sigma^2_{\mathrm{x}_*})$$

where

$$\begin{aligned} \mu_{\mathrm{x}_*} &= k_*^T (K + \sigma_n^2 I)^{-1} y \\ \sigma^2_{\mathrm{x}_*} &= k(\mathrm{x}_*, \mathrm{x}_*) - k_*^T (K + \sigma_n^2 I)^{-1} k_* \end{aligned} \tag{5}$$

Here k_* is an n-dimensional column vector, describing the covariances between x_* and the n training inputs X, and K is the covariance matrix of the inputs X.

At the end of the modeling step, we get several intensity distribution maps including the mean fields and the corresponding variance fields, regarding each LED light source. They supply the key references of the observation model for Bayesian dynamic deduction. A pair of example results is shown in Fig. 4. The regression mean represents the expected light signal observation; the variance field represents the observation likelihood. The "shape" of the variance field roughly represents the traversable areas, since the observations over these areas are with higher confidence and thus low covariance values. For the same reason, the variance field could directly used for path-planning which will be discussed later.

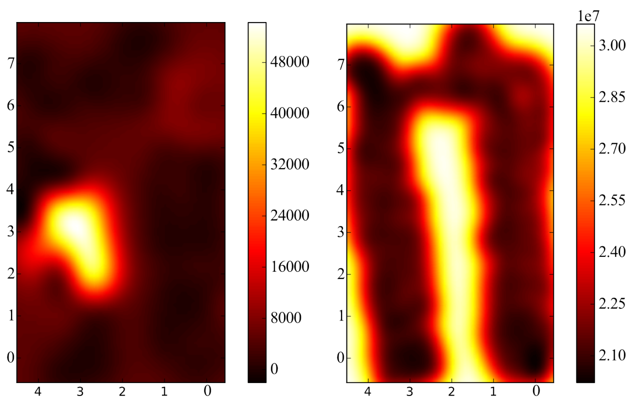

(a) The mean field of light source 6 (b) The variance field of light source 6

Fig. 4. A typical example of the Gaussian Process results

V. Path-planning Algorithm

The realization of path-planning depends on precise localization and map construction. Precise map construction requires metric information provided by a SLAM system, which is usually a costly way. While a metric-free solution is proposed based on the previous environment modeling results.

A. Cost Map Construction

First of all, we need to construct a cost-map including nodes and arcs in the VLC environment. The map generated by the robot is naturally the first choice. However, in general cases, the map calculated has a noisy boundary. More importantly, it is coupled with dynamic objects in the mapping process. This means a pre-denoising step is needed. Comparatively, the variance field computed by the Gaussian Process is a better choice since it naturally provides references regarding the trust to the original data. A sample variance field is shown in Fig. 6 (a). Besides this, it is also applicable under other test conditions where laser range finders may not even be available at all, e.g. the ground-truth may be provided by a motion tracking system.

Specifically, the nodes represent the discrete locations in the real world while the arcs denote the connection relationship between nodes. Usually the map is represented by a pixel-based picture so every node has eight neighboring nodes except the marginal ones, which is shown in Fig. 5 (a). There are two statuses of the nodes, 'free' for the nodes located in the traversable area and 'obstacle' for the nodes otherwise. The arcs here are directional, namely there are two arcs between every two nodes. Each arc has an associated cost value. A cost could be defined to be distance, energy expended, time exposed to danger, etc. In our work, we simply define the cost to be uniform in traversable areas since isotropy is a reasonable assumption in the indoor environment. Given the cost graph, the next step is to find the minimum total cost path from the start node(S) to the goal node(G) based on a search algorithm. In our demo, the current position is obtained from the VLC-based localization while the goal position is manually defined. A sampled path is shown in Fig. 5 (b).

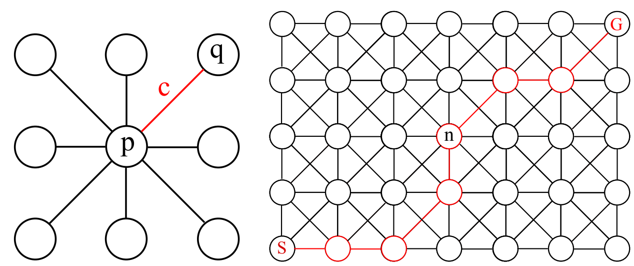

(a) nodes and arcs (b) path generated by the search algorithm

Fig. 5. Cost graph and a sample path within an image-form map

We first apply a binarization step on the variance field. Then, the planning is implemented using only the binary version. A sample of the raw variance field and the binarization results are shown in Fig. 6(a) and (b), respectively.

In practice, the suggested path ought not to hit on the boundary of the obstacle considering collision volume. In order to keep a safe distance from the obstacles, an expanding process is applied to the obstacle area, which is shown in Fig. 6(c). Euclidean distance is used to construct the cost map for free nodes, and positive infinity for obstacles. A sample path on the variance field is shown in Fig. 6(d).

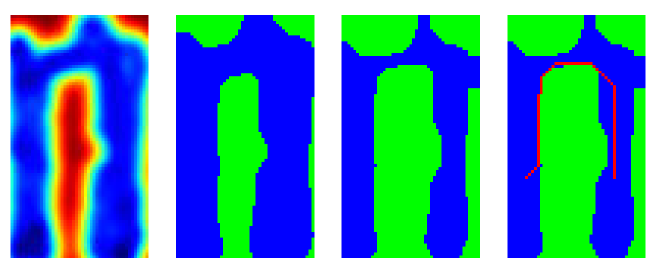

(a) Variance field (b) Binarization (c) Securing (d) Path

Fig. 6. Steps for path-planning

B. Algorithm

Dijkstra's algorithm is a widely used graph-search method to find the shortest path based on non-negative edge costs. Compared with the Dijkstra's algorithm, A* is a smarter method integrated with an evaluation function $\hat{f(n)}$ to determine which node should be visited next. For any starting node S and goal node G, $f(n)$ is defined as the actual cost of an optimal path which is constrained to go through node n (refer to Fig. 5 (b)), it could be written as the sum of two parts:

$$f(n) = g(n) + h(n)$$

$\hat{h(n)}$:	0(Dijkstra's)	$(x+y)/2$	$\sqrt{x^2+y^2}$	$max(x,y) - min(x,y) + \sqrt{2} * min(x,y)$
Length(m)	9.7456	9.7456	9.7456	9.7456
Time(ms)	23	34	**22**	26
Length(m)	10.671	10.671	10.671	10.671
Time(ms)	48	70	**38**	54

TABLE I
THE COMPARISON OF DIFFERENT ALGORITHMS

Algorithm for path-planning based on the variance field by GP
1. Variance field binarization and refinement the 'free' and 'obstacle' areas are then determined 2. Cost map construction: for each pair of neighboring node p and node q a. if both p and q are located in 'free' area: $C_{pq} = \|A_{pq}\|$ b. else: $C_{pq} = +\inf$ 3. Set $p = S$, the start point and calculate $\hat{f(p)}$ 4. Expand p as follows: if $p == G$, mark p CLOSED and end the algorithm else mark p CLOSED and: for each of p's neighbors q that are not expanded a.calculate $\hat{f}$ for q if $\hat{f(q)}$ decreased, make q point back to p b.mark q ACTIVE if q has never been visited or $\hat{f(q)}$ is smaller now than it was marked CLOSED 5. Set r = node with minimum evaluation function on the ACTIVE list: 6. Repeat Step 2 for $p = r$ 7. Visualization

[1] The A_{pq} denotes the real distance between node p and node q.

TABLE II
PATH-PLANNING ALGORITHM

where $g(n)$ is the cost of the best path so far from S to n, and $h(n)$ is the estimated cost of an optimal path from n to G. In practice, we only need to know the estimation of $f(n)$ as the sum of the estimations of $g(n)$ and $h(n)$ is

$$\hat{f(n)} = \hat{g(n)} + \hat{h(n)}$$

The optimal choice of $\hat{g(n)}$ is the cost of the path from S to n, the minimal cost so far. The selection of $\hat{h(n)}$ depends on the physical information in the real problem. In this work, it is defined as the distance from n to G in the variance field. Actually $\hat{h(n)}$ is the source of the heuristic factor of the algorithm that ensures the algorithm always firstly expands the most likely node in the shortest path. It has been proved that A* is not only admissible but optimal if the evaluation function $\hat{h(n)}$ satisfies a certain requirement [10]. Here 'admissible' means A* is guaranteed to find an optimal path from a start node to a preferred goal node, and 'optimal' means the total cost of the expanded nodes in the algorithm is minimized.

Dijkstra's algorithm can be actually regarded as a particular case of the A* algorithm with the heuristic item $h(n)$ being constantly 0. Compared with the time complexity of Dijkstra's algorithm, A* seems to have an overwhelming advantage, however, the optimal heuristic function is hard to achieve and the complexity of the calculation of the heuristic item usually is not a small expense. Thus we need to balance the complexity and the heuristic effectiveness of $\hat{h(n)}$ to obtain a reasonable solution according to the application. The overall path-planning algorithm on the variance field of the GP model in the VLC-based system is shown in Table II.

The path planning function is realized on a tablet with a photonic diode connected to the tablet through a USB sound card. The user interface is shown in Fig. 7. The performance is shown by the supplementary video.

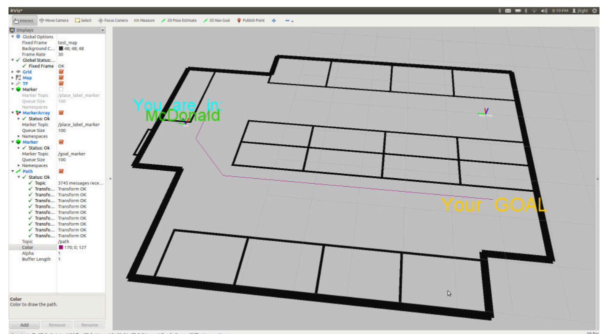

Fig. 7. The Rviz-based user interface of the localization and path-planning system

C. Validation and Experiment

In order to compare different path-planning algorithms, we conducted experiments in the same indoor environment as that for the localization test. Considering the admissibility condition, we chose 0, $(x+y)/2$, $\sqrt{x^2+y^2}$ for comparison, in which 0 corresponds to the Dijkstra's algorithm. $\sqrt{x^2+y^2}$ corresponds to the most reasonable heuristic method since it represents the direct distance in the 2D plane, the number of the expanded nodes is minimized but the computation complexity of each node is considerable. While $(x+y)/2$ will expand more nodes but the total computation complexity may be reduced. Besides these three choices, we let $\hat{h(n)}$ be $max(x,y) - min(x,y) + \sqrt{2} * min(x,y)$ to further meet the practical situation.

The map resolution is set to be 10 centimeters. We use a fixed start point and the goal point to perform the algorithm comparison (the debug mode). The comparison is made on the map based on the variance field. As we can see from Fig. 8, all the algorithms with different heuristic items can compute paths from the start to the goal with marginal differences. The quantitative results are shown in Table I, in which 'Length' represents the length of the generated path and 'Time' denotes the computation time a certain search assignment needs, which reflects the total computation efficiency. As we can see from the experiment data, all the alternatives can find a optimal path but $\sqrt{x^2+y^2}$ has the most stable performance of all. The fourth choice $max(x,y) - min(x,y) + \sqrt{2} * min(x,y)$ is the graph representation of the point-to-point distance $\sqrt{x^2+y^2}$, thus the path-planning result is quite similar with the Dijkstra's.

The path-planning algorithm is then applied on a tablet with the heuristic item $\sqrt{x^2+y^2}$ to realize real-time path-planning and re-planning. The real-time demo shows the path-planning result is still acceptable even thought the operating height and orientation are not stable(hand-held case with acceptable orientation change). For further details, please refer to the attached video.

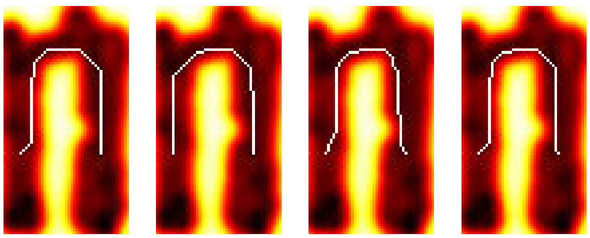

Fig. 8. Sample path-planning results based on different heuristic items, the corresponding values of $\hat{h(n)}$ from left to right are 0, $(x+y)/2$, $\sqrt{x^2+y^2}$ and $max(x,y) - min(x,y) + \sqrt{2} * min(x,y)$

VI. Conclusion

In this paper, we proposed an environment modeling-based metric-free path-planning solution using a VLC-based system. We applied Gaussian Process Regression to solve the environment modeling problem. We compared different A* algorithms for path-planning through experiments on the variance field that derived from the Gaussian Process Regression. The results showed the accuracy and practicality of our system, which tends to be a better solution for indoor localization and path-planning with minor requirements on hardware and computation, for both robotic applications and personal positioning applications. In the future, we want to further improve the accuracy and robustness of the system in terms of the training method of the Gaussian Process.

Video Supplement

The attached video shows the real-time path-planning results. Note that we mimic an environment of a big shopping mall and demonstrate our indoor localization and path-planning system on the tablet. Different regions in the map are decorated with commercial brands to vividly demonstrate the idea for indoor positioning-based services. The user is moving in the test environment with a hand-held tablet. The screen-shots of the path-planning results and two real views are simultaneously presented. Note that the tablet can potentially be replaced by other devices with photonic diodes, e.g. most smart-phones with approximation sensors, etc.

References

[1] L. Wang, M. Liu, and M. Q.-H. Meng, "Real-time multisensor data retrieval for cloud robotic systems," *Automation Science and Engineering, IEEE Transactions on*, vol. 12, no. 2, pp. 507–518, 2015.

[2] M. Montemerlo, S. Thrun, D. Koller, and B. Wegbreit, "FastSLAM: A factored solution to the simultaneous localization and mapping problem," in *AAAI/IAAI*, 2002, pp. 593–598.

[3] M. Liu and R. Siegwart, "Dp-fact: Towards topological mapping and scene recognition with color for omnidirectional camera," in *Robotics and Automation (ICRA), 2012 IEEE International Conference on*. IEEE, 2012, pp. 3503–3508.

[4] M. Liu, C. Pradalier, F. Pomerleau, and R. Siegwart, "Scale-only visual homing from an omnidirectional camera," in *Robotics and Automation (ICRA), 2012 IEEE International Conference on*. IEEE, 2012, pp. 3944–3949.

[5] M. Liu, C. Pradalier, and R. Siegwart, "Visual homing from scale with an uncalibrated omnidirectional camera," *Robotics, IEEE Transactions on*, vol. 29, no. 6, pp. 1353–1365, 2013.

[6] M. Liu, D. Scaramuzza, C. Pradalier, R. Siegwart, and Q. Chen, "Scene recognition with omnidirectional vision for topological map using lightweight adaptive descriptors," in *Intelligent Robots and Systems, 2009. IROS 2009. IEEE/RSJ International Conference on*. IEEE, 2009, pp. 116–121.

[7] M. Liu, K. Qiu, S. Li, F. Che, L. Wu, and C. P. Yue, "Towards indoor localization using visible light communication for consumer electronic devices," in *Proceedings of the IEEE/RSJ International Conference on Intelligent Robots and Systems (IROS)*, Chicago, the USA, 2014.

[8] F. Zhang, K. Qiu, and M. Liu, "Asynchronous blind signal decomposition using tiny-length code for visible light communication-based indoor localization," in *Proceedings of the IEEE International Conference on Robotics and Automation (ICRA)*, 2015.

[9] E. W. Dijkstra, "A note on two problems in connexion with graphs," *Numerische mathematik*, vol. 1, no. 1, pp. 269–271, 1959.

[10] P. E. Hart, N. J. Nilsson, and B. Raphael, "A formal basis for the heuristic determination of minimum cost paths," *Systems Science and Cybernetics, IEEE Transactions on*, vol. 4, no. 2, pp. 100–107, 1968.

[11] F. Colas, S. Mahesh, F. Pomerleau, M. Liu, and R. Siegwart, "3d path planning and execution for search and rescue ground robots," in *Intelligent Robots and Systems (IROS), 2013 IEEE/RSJ International Conference on*. IEEE, 2013, pp. 722–727.

[12] M. Liu and R. Siegwart, "Navigation on Point-cloud - a Riemannian Metric approach," in *IEEE International Conference on Robotics and Automation (ICRA)*, 2014.

[13] A. Stentz, "Optimal and efficient path planning for partially-known environments," in *Robotics and Automation, 1994. Proceedings., 1994 IEEE International Conference on*. IEEE, 1994, pp. 3310–3317.

[14] A. Stentz *et al.*, "The focussed d* algorithm for real-time replanning." in *IJCAI*, vol. 95, 1995, pp. 1652–1659.

[15] S. Koenig and M. Likhachev, "Fast replanning for navigation in unknown terrain," *Robotics, IEEE Transactions on*, vol. 21, no. 3, pp. 354–363, 2005.

[16] M. Liu, "Robotic online path-planning on point-cloud," *IEEE Transactions on Cybernetics*, no. CYB-E-2015-01-0021.

[17] X.-W. Ng and W.-Y. Chung, "Vlc-based medical healthcare information system," *Biomedical Engineering: Applications, Basis and Communications*, vol. 24, no. 02, pp. 155–163, 2012.

[18] M. Abualhoul, M. Marouf, O. Shagdar, F. Nashashibi *et al.*, "Platoon control using vlc: A feasibility study." 2013.

[19] E. Poves, G. del Campo-Jimenez, and F. Lopez-Hernandez, "Vlc-based light-weight portable user interface for in-house applications," in *Consumer Communications and Networking Conference (CCNC), 2011 IEEE*. IEEE, 2011, pp. 365–367.

[20] G. del Campo-Jimenez, J. M. Perandones, and F. Lopez-Hernandez, "A vlc-based beacon location system for mobile applications," in *Localization and GNSS (ICL-GNSS), 2013 International Conference on*. IEEE, 2013, pp. 1–4.

[21] T. Tanaka and S. Haruyama, "New position detection method using image sensor and visible light leds," in *Machine Vision, 2009. ICMV'09. Second International Conference on*. IEEE, 2009, pp. 150–153.

[22] M. Yoshino, S. Haruyama, and M. Nakagawa, "High-accuracy positioning system using visible led lights and image sensor," in *Radio and Wireless Symposium, 2008 IEEE*. IEEE, 2008, pp. 439–442.

[23] H.-S. Kim, D.-R. Kim, S.-H. Yang, Y.-H. Son, and S.-K. Han, "An indoor visible light communication positioning system using a rf carrier allocation technique," *Journal of Lightwave Technology*, vol. 31, no. 1, pp. 134–144, 2013.

[24] C. E. Rasmussen, "Gaussian processes for machine learning," 2006. [Online]. Available: http://www.gaussianprocess.org/gpml/chapters/RW.pdf